Numerical investigation of the behavior of stone ballast mixed by steel slag in ballasted railway track

Jing, Guoqing; Wang, Jingru; Wang, Haoyu; Siahkouhi, Mohammad

DOI
10.1016/j.conbuildmat.2020.120015

Publication date
2020

Document Version
Accepted author manuscript

Published in
Construction and Building Materials

Citation (APA)
Jing, G., Wang, J., Wang, H., & Siahkouhi, M. (2020). Numerical investigation of the behavior of stone ballast mixed by steel slag in ballasted railway track. *Construction and Building Materials*, *262*, Article 120015. https://doi.org/10.1016/j.conbuildmat.2020.120015

Numerical investigation of the behavior of stone ballast mixed by steel slag in ballasted railway track

Guoqing Jing [a], Jingru Wang [a], Haoyu Wang [b], Mohammad Siahkouhi [a*]

[a] Civil Engineering School, Beijing Jiaotong University, Beijing 100044, China

[b] Engineering Structures Department, Delft University of Technology, the Netherlands

Abstract

Recently, implementing steel slag ballast has been proposed as an appropriate material to substitute stone ballast. In this regard, one of the technical concerns is the behavior of steel slag ballast in both time and frequency domains that needs to be assessed, properly. Furthermore, the combination of stone ballast and steel slag is unavoidable in steel slag ballasted tracks during track maintenance concerning the limitation of steel slag resources. Therefore, this paper suggests an optimal stone ballast-steel slag (SB-SS) combination regarding the dynamic behavior of five SB-SS combinations as 0%SS, 25%SS, 50%SS, 75%SS and 100%SS by weight of ballast using a finite element method (FEM) model of a 50-meter test track. Moreover, using elasticity modulus and Moher-coulomb parameters obtained via a series of plate load and shear strength tests for each SB-SS combination turns FEM model to be more close to the real test track results.

Experimental results show that adding steel slag particles to stone ballast increases elasticity modulus and friction angle of ballast layer resulting in the improvement of mechanical

* (Corresponding author)
Email: mohammad.siahkouhi@gmail.com

behavior of railway track. Consequently, the maximum deflections and root mean square (RMS) of accelerations decrease by increasing steel slag content. Analyzing free vibration of ballast layer combinations reveals that damping ratios of 100%SS ballast layer is the maximum value as 0.25 followed by 75%SS, 50%SS, 25%SS and 0%SS combinations. Moreover, the dominant frequencies of each ballast layer combinations determine that 0%SS, 25%SS and 50%SS coincides within the track excitation frequency range made by wheel sets, while 75%SS and 100%SS are out of which. Finally, according to all results, 75%SS ballast layer is proposed as the optimal SB-SS combination.

Keywords: Plain ballasted railway track; Finite element method; Steel slag; Mohr-Coulomb parameters; Sustainable design

1. Introduction

Ballasted railway tracks contain five main components as rails, fasteners, sleepers, ballast layer and subgrade. Ballast layer is important, as it supports sleepers, transfers dynamic loads to the subgrade and provides sufficient drainage [1]. Therefore, ballast as a part of the main components of railway tracks, always attracts attention. One of the ballast layer properties that can provide some of the features mentioned above depends on ballast particles' material type that effects on the overall performance of this layer [2]. Typically, the ballast layer consists of stone; however, some modification methods or replacement materials for stone ballast are proposed that can be seen in Table. 1.

Table. 1. Materials suggested to be used as ballast particles.

No.	Researcher	Year	Material	Results

1	G. Jing et al. [3]	2019	Recycled ballast	• The reduction of shear strength and coordination number of the mixture is not considerable, when mixed with less than 30% recycled ballast.
2	Delgado et al. [4]	2019	Steel slag	• The steel slag aggregate has higher values of strength parameters and long-term deformability compared to the granite aggregate and better behavior in particle breakage.
3	Esmaeili et al. [5]	2017	Tire derived aggregate (TDA) (Ballast mixture)	• The 5%-TDA mixed with ballast was determined as the most suitable mixture in terms of breakage and stiffness.
4	Solsanchez et al. [6]	2018	Neo ballast (natural aggregates coated with rubber particles)	• Neo ballast allows for higher damping capacity, reduction in stress, and lower long-term settlement and vertical stiffness.

Recently, many countries such as Iran, Japan, Australia, Europe, USA and China have a massive amount of steel slag, the annual production rate of which is around 2.2 [2], 13.5 [7], 3.4 [8], 45 [9], 16 [10] and 100 million tons [11], respectively. The utilization of steel slag has been propounded in various parts of railway tracks, such as ballast, sub-ballast and subgrade, because of the financial issue, recycling of the waste material and positive impacts on the environment. For instance, the steel slag has been used in the part of Hassan Abad–Diziche railway line in the Isfahan province, Iran [2], Toronto–Montreal railway line in Canada [12], the major part of Western mainline near the California–Nevada border in the US [13], as well as in Brazil [14] and Portugal [4].

Kaya researched the stress-strain behavior of railroad ballast materials using of parallel gradation technique. Internal friction angle and apparent cohesion of ballast were taken into account as 42 and 32 kPa. The plastic strain of steel slag was investigated, and its result was as 0.75 [15]. Delgado et al. researched steel slag particles to be used as ballast resources. It was proved that steel slag particles have more strength against cyclic loading, long-term deformability behavior and lower degradation and particle breakage compared to granite

ballast [4]. Esmaeili et al. investigated lateral resistance of railway track with steel slag and limestone as ballast particles. The results showed that a 27% increase in lateral resistance of track with steel slag ballast respect to that of limestone ballast [16]. In another research by Esmaeili et al., abrasion characteristics of steel slag and granite ballast were compared. The results showed that Los angles and Micro-Deval index of steel slag particles proportion to granite ballast are 2.5 and 0.75, respectively [17]. Vertical load distribution on steel slag ballast compared to limestone ballast was studied in experimental research by Esmaeili et al. It was proved that the rail support modulus of the test track with steel slag is 1.64 times higher than that of limestone ballast, and the compressive contact pressure of sleeper and ballast in limestone ballast was almost 1.39 times greater than steel slag ballast [2]. Sahay et al. proposed many applications for steel slag as aggregate and ballast layer implementation with respect to its physical properties [18]. Koh et al. investigated the performance of steel furnace slag as ballast material in railway track. The effects of the ageing period were studied in 3 and 6 months. It was concluded that the physical and chemical properties of the steel furnace slag within 3 and 6 ageing periods satisfy all requirements of standards [19]. Dhoble et al. reviewed the application of steel slag in bituminous mixes, cement ingredient and as concrete aggregate, antiskid aggregate, and railroad ballast. It is proposed to use slow cooled steel slag in the railroad ballast [20]. Oluwasola et al. studied the application and characteristics of steel slag. The main chemical composition of steel slag consisted of CaO, SiO_2, MgO and etc. Finally, it is proposed to use this material in civil engineering projects [21]. Wang et al. reported that the Los Angeles abrasion index of steel slag is under 30% [22].

A new challenge has arisen in the time being as limited resources of steel slag corresponding to the high volume ballast materials that are needed to implement a ballasted railway track.

Generally, to implement a 1 km ballasted track (35 cm deep ballast, concrete sleeper, straight line, and 40 cm width ballast shoulder) almost 2000 tons ballast material is needed. This means using a simple calculation according to annually steel slag production rate in countries of Iran, Japan, Australia and China after almost 1000 km, 6500 km, 1700 km, and 50000 km one line railway track implementation, respectively, all the restored resources of steel slag will be consumed and its production is insufficient that results in railway track owners wait sometimes for being supplied by steel slag materials. This should be considered that it is assumed that all the produced steel slag is suitable regarding size and shape to be used as ballast particles [23]. Therefore, in order to the railway track maintenance, the combination of steel slag and stone ballast is unavoidable. That can happen due to not available steel slag material while it is needed to be used for adjusting track elevation or track renewal. Here is the challenge that is considered as the main target of the current research.

To evaluate the combination behavior of steel slag and stone ballast, numerical modelling is conducted supported by the experimental investigation. The numerical modelling method is proved over the year that can be a trustful tool to evaluate railway tracks behaviors [24, 25]. The numerical parameters (Mohr-Coulomb inputs) that improve the modelling accuracy are obtained from a series of shear strength and plate loading tests. The shear strength tests for ballast particles are researched by [3, 26-30] that can prove its compatibility for obtaining Moher-Coulomb parameters of ballast particles.

None of the aforementioned studies has addressed the dynamic behavior of a mixture of steel slag and stone ballast. Here five types of combination of steel slag and stone ballast (SS-SB)

are considered, including 0%, 25%, 50%, 75% and 100% by weight of ballast. Firstly, the elasticity modulus and Moher coulomb parameters of each proposed combination are obtained and compared. Then a comparative numerical investigation is conducted, and the rail displacement, sleeper acceleration, damping ratios and dominant frequency of track are studied in five FEM models. Finally, according to the results the optimal combination is proposed to be implemented in railway track.

2. Experimental study

2.1. Materials specifications

The test plan in this research consisted of two kinds of materials as basalt stone and steel slag. Basalt ballast is one of the popular granular materials which mostly is used for the ballast layer in many countries. The steel slag is supplied by the Lingshou town Xinfu mineral company's products which are derived from steel production procedure by electric arc furnace method. The current steel slag is separated from melted steel after its purification process. The gradation curves of basalt and steel slag ballast are shown in Fig. 1 according to AREMA standard grade 3 [31]. Table 2 shows the mechanical specifications for both types of ballast which have been measured via a series of laboratory tests for all five SS-SB combinations according to American society for testing and materials (ASTM).

As can be observed, the results of the Los Angles test confirm that the abrasion resistance of stone ballast is higher than that of steel slag, although both of them are within the allowable limit (<18%) [3]. Based on these preliminary specifications, the less reduction in track

settlement, sleeper acceleration and dominant frequency is predicted under various combinations of SB-SS.

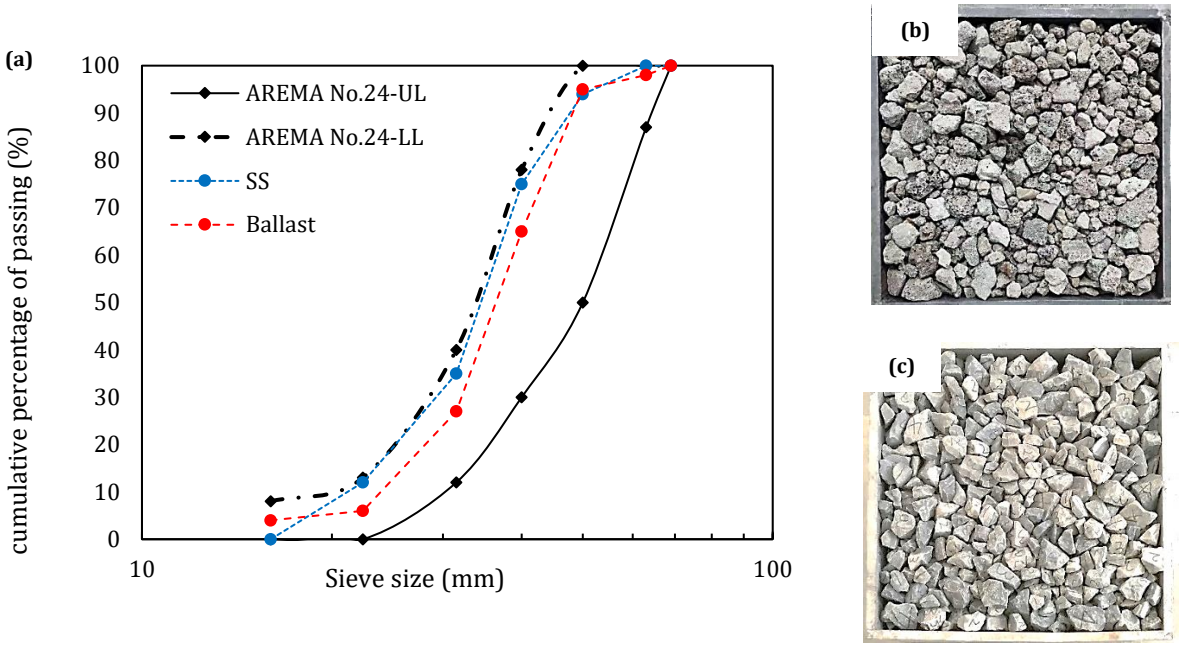

Fig. 1. **(a)** Gradation curves of SS and SB and, an overview of **(b)** steel slag and **(c)** basalt ballast particles.

Table. 2. Basalt and steel slag specifications.

Feature	Unit	Basalt stone	25%SS	50%SS	75%SS	100%SS	Standard test method
Water absorption	%	0.6	0.76	0.77	0.79	0.8	ASTM C127
Granular density	(g/cm^3)	2.81	2.81	2.94	3.06	3.4	
Los angles index	%	9.94	10.99	11.32	14.77	16.5	ASTM C-131-96

2.2. Elasticity modulus

By applying the elasticity theory, the elastic settlement of the rigid circular loading plate with the diameter of *D* can be calculated using Equation (1) proposed by Timoshenko and Goodier [32]. This equation is based on the Boussinesq theory (1885) [33], which defines the

relationship between the settlement of a rigid circular plate and corresponding normal stress applying on a homogeneous space.

$$E_s = \frac{\pi \times q \times D}{4s}(1 - \upsilon^2) \quad (1)$$

Where E_s, q, s, υ and D denote elastic modulus, average normal stress, settlement of the plate associated with the pressure, Poisson's ratio, and the circular plate diameter, respectively. Therefore, by substituting the ballast layer settlement of the plate loading test (see Fig. 2), with respect to the maximum loading stress, the ballast layer elasticity modulus can be obtained as Table. 3. It should be noted that the Poisson's ratio of ballast layers are considered as 0.4 in elasticity modulus computation.

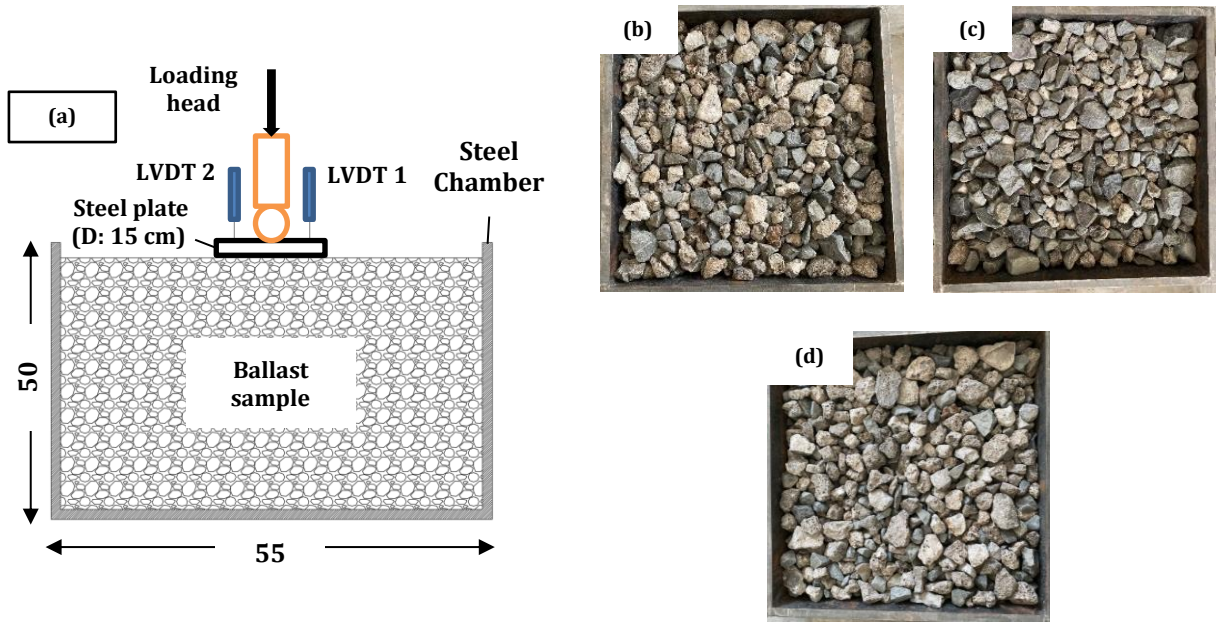

Fig. 2. A schematic overview of **(a)** plate loading test apparatus and specimens including **(b)** 25%SS, **(c)** 50%SS and **(d)** 75%SS.

Table. 3. Elasticity modulus of SS-SB combinations.

Parameters	Unit	0%SS	25%SS	50%SS	75%SS	100%SS
Elasticity modulus	(MPa)	157	168	172	177	180

2.3. Mohr-Coulomb parameter

By conducting a series of shear strength tests on 0%SS, 25%SS, 50%SS, 75%SS and 100%SS specimens, the Mohr-Coulomb parameters of each specimen, including friction angle, are extracted. The large-scale direct shear apparatus consists of two boxes as shown in Fig. 3. The upper box is 600 mm × 600 mm × 300 mm, and the lower box is 600 mm × 700 mm × 250 mm. Totally, fifteen specimens were prepared with 0%SS, 25%SS, 50%SS, 75%SS and 100%SS to obtain internal friction angle of steel slag mixed by stone ballast particles under 50 kPa, 100 kPa and 200 kPa normal stresses. Table. 4 shows the Mohr-Coulomb parameters of each steel slag fraction specimen. It can be concluded that the steel slag association increases the internal friction angle of the ballast layer. The internal friction angle of the steel slag ballast is more than basalt ballast, which causes more inter-particle interlocking mobilization and leads to better stress distribution in comparison to basalt ballast.

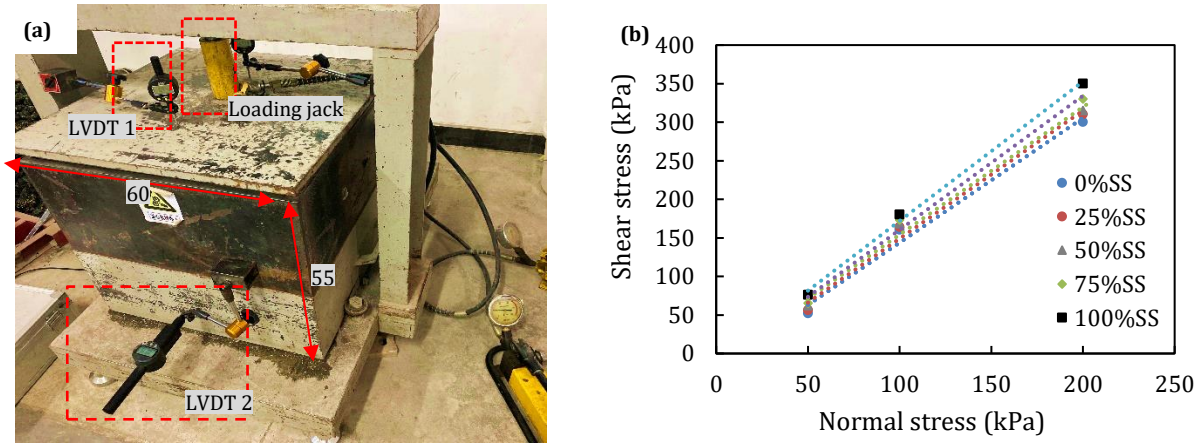

Fig. 3. An overview of **(a)** shear strength test apparatus and dimension (cm) and **(b)** Moher-Coulomb parameters result.

Table. 4. Mohr-Coulomb specification of SS-SB combinations.

parameter	Unit	0%SS	25%SS	50%SS	75%SS	100%SS

Friction angle	(°)	40.5	41	42.5	44	46

3. Numerical study

3.1. FEM model and verification

In this section, a FEM model of 50 m plain railway track is developed consisting of UIC 60 rails, wooden sleepers, ballast layer and subgrade. The numerical model is validated against the results of field tests in Ref. [2]. The properties of the track components and loadings in Ref [2] are used. A general static analysis was performed using 130 kg wagon and 30 kg one as high weight and lightweight trains. The corresponding maximum deflections for two wheels are shown in Fig. 4. Accordingly, the rail support modulus can be obtained using Talbot equation [34, 35] with measuring the area of deflection basin between the heavy train and lighter one (See Eq. 2). Both tracks with 100% steel slag ballast and 100% stone ballast results are used for validating FEM models which are in a good agreement with the field results (Table. 5).

$$K = \frac{\sum P_2 - \sum P_1}{A} \tag{2}$$

Where P_2 and P_1 are heavy and the light car weights (kN) and A refers to the area of deflection basin between two types of loads, respectively.

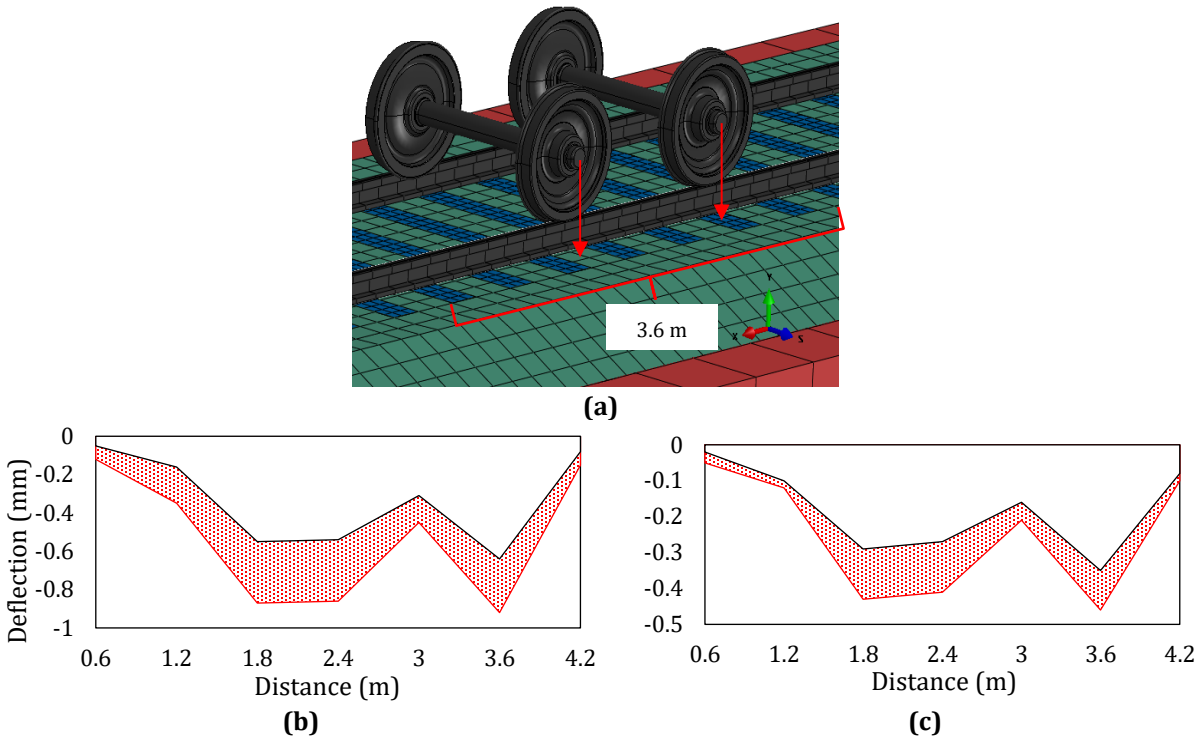

Fig. 4. **(a)** the modeling of two wheels to obtain deflection of sleepers, and sleepers' vertical deflection basin (highlighted red) according to light weight (30 kg) and heavy weight (130 kg) trains loading for **(b)** 0%SS and **(c)** 100%SS.

After validation of 0%SS and 100%SS ballasted railway track models using field data, their dynamic results are obtained and reported. The dynamic behavior of remained three combinations, including 25%SS, 50%SS and 75%SS, are calculated using the validated models just by changing the ballast layer properties according to experimental results. The dynamic loading is modelled as the gas turbine 26 (GT26) diesel with 11.25 tons wheel load as shown in Fig. 5 [12]. Afterwards, the dynamic results were presented and compared, including rail displacement, sleeper acceleration, ballast damping ratios and track frequencies at 25-m of track distance.

Table. 5. The difference between FEM and field results.

Ballast layer		100%SS	Difference (%)	0%SS	Difference (%)
Rail support modulus (MPa)	Field	100	2	61	1.6
	FEM	103		62	

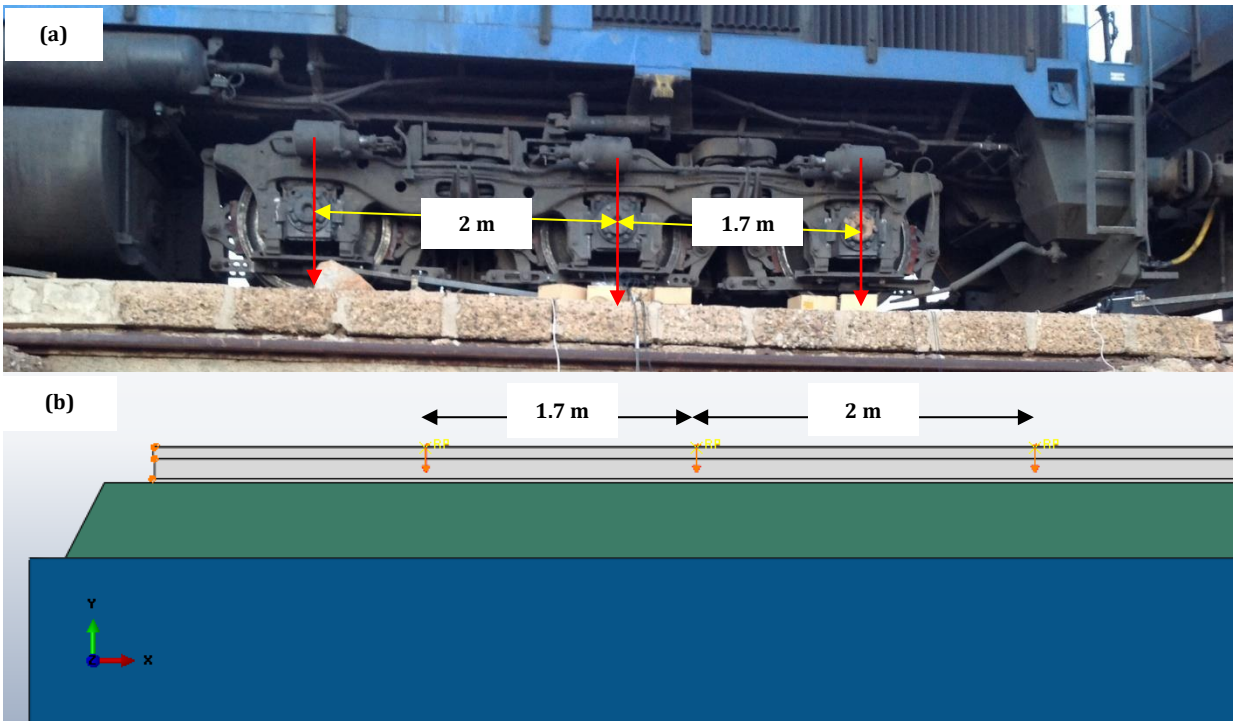

Fig. 5. The loading pattern of **(a)** GT diesel and corresponding loading placement of **(b)** FEM model.

A three-dimensional linear and Moher-Coulomb model is developed by the finite element software Abaqus [36]. The loading is considered as moving reference (RF) points at 100 km/h, which is the normal speed of GT trains. The track superstructure consists of UIC 60 rails, wooden sleepers, ballast layer (30 cm thickness) and subgrade. Ballast layer is modeled as deformable solid that its parameters are assigned as density, elasticity modulus, Moher coulomb parameters and Poisson's ratio, the same modeling method is performed in Refs. [25, 37, 38]. All components of the ballasted railway track are discretized using structured

hexahedral elements and the mesh size of 10 cm for the wooden sleeper, 20 cm for the rails and ballast layer and 60 cm for subgrade as shown in Fig. 6. It should be notified that a sensitivity analysis had been done on track stress value to optimize the mesh size of track components. Table. 6 shows the track components specification used for FEM modeling. Subgrade, wooden sleeper and rails specifications are extracted from literature reviews [2, 25, 37], while ballast layers' properties are obtained from experiments that are mentioned above as elasticity modulus and Moher coulomb parameters. Density of ballast layer for each combination obtained using ballast bulk density test accordance with AS 1141.4 [39].

Table. 6. The specifications of track's components.

Material properties	Subgrade	Ballast					Wooden sleeper	Rails
		0%SS	25%SS	50%SS	75%SS	100%SS		
Material model		Moher-coulomb					Linear elastic	
Density (g/cm^3)	1.8	1.5	1.67	1.82	1.91	2.1	1.01	7.85
Elasticity modulus (MPa)	45	157	168	172	177	180	14000	210,000
Friction angle (°)	30	40.5	41	42.5	44	46	-	-
Cohesion (kPa)	50			2			-	-
Poisson's ratio	0.33			0.4			0.45	0.3

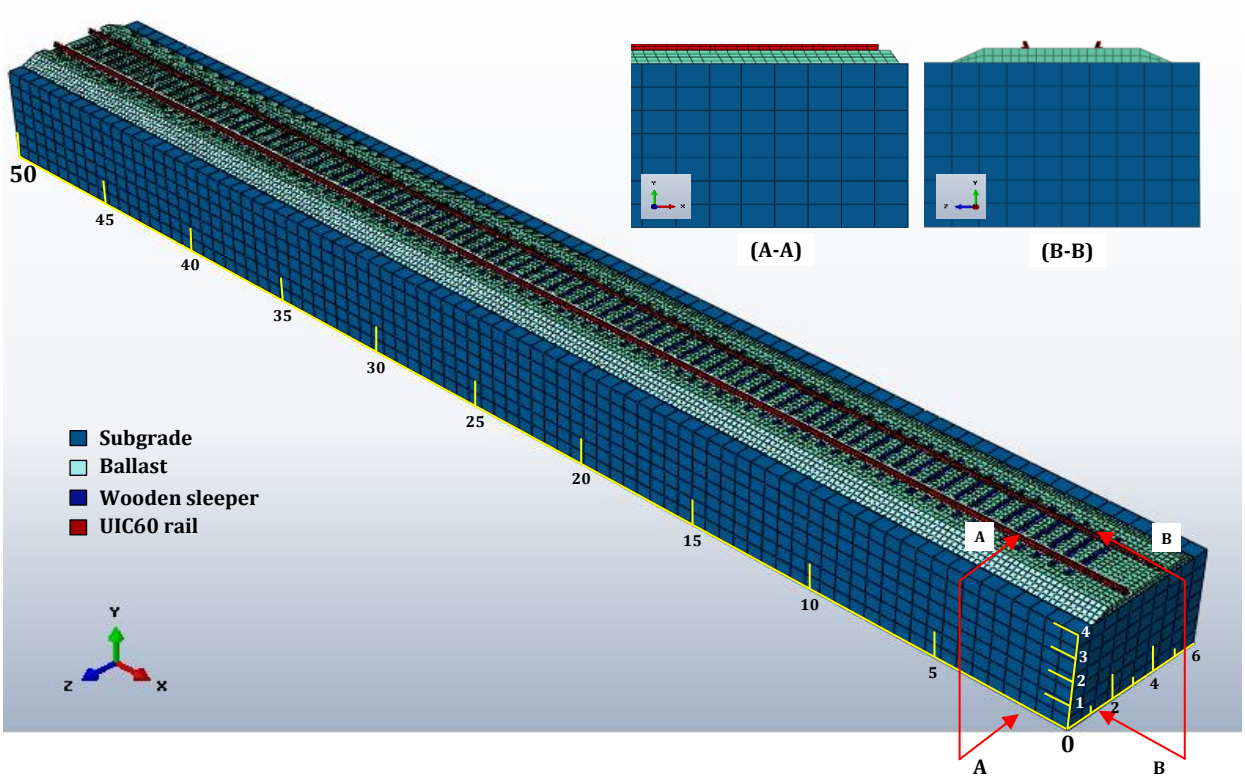

Fig. 6. An overview of the FEM model dimensions (m) and components layout.

3.2. Time domain

In order to perform a comprehensive analysis of five different ballast layers with steel slag content, four parameters of railway track are studied, including track deflection, sleeper acceleration, ballast damping ratios and track dominant frequency. It should be noted that all the parameters are presented for vertical measurement and at 25 m distance of the track as can be seen in Fig. 7.

3.2.1. Track vertical deflections

Fig. 8 shows the vertical deflection railway track in the x-y plane and A-A section at 25 m distance. As can be seen, the deflections of track components decrease by increasing steel slag content. Considering surface deflections of ballast layers for 25%SS, 50%SS, 75%SS and

100%SS compared to the combination of 0% SS, their values decrease by 24%, 30%, 30% and 51%, respectively. These decrease percentages in deflections are due to the higher value of Moher-Coulomb parameters of ballast layers with steel slag content. High deflection of railway track components lead to the compaction of ballast and more ballast particles abrasion that causes shorter track maintenance periods and increasing cost [40].

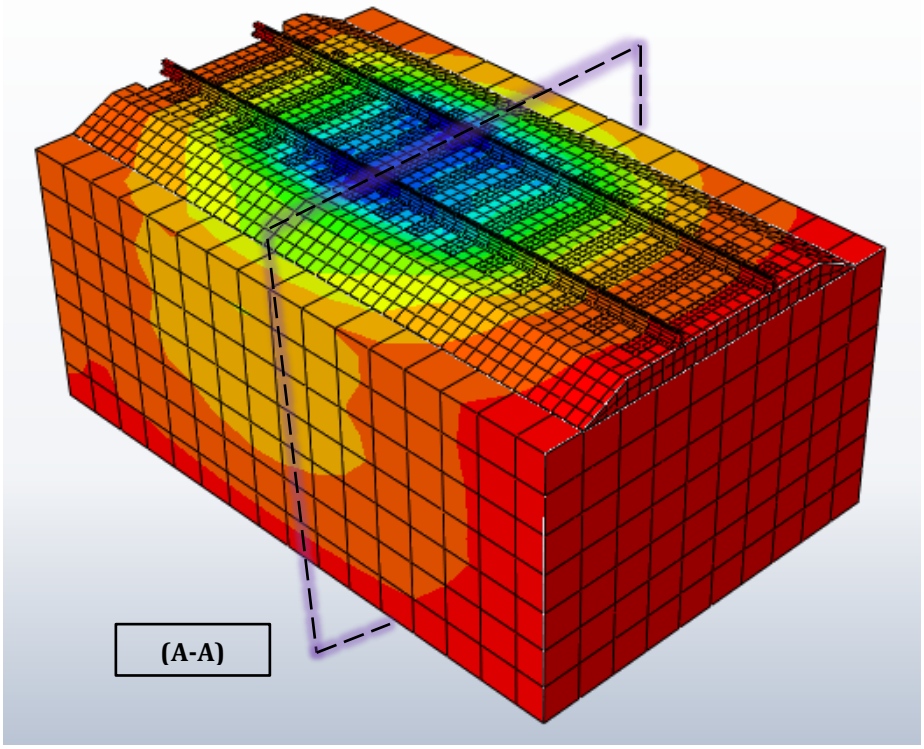

Fig. 7. The effects of train load on the vertical displacement of ballast railway track and the (A-A) section of showing results.

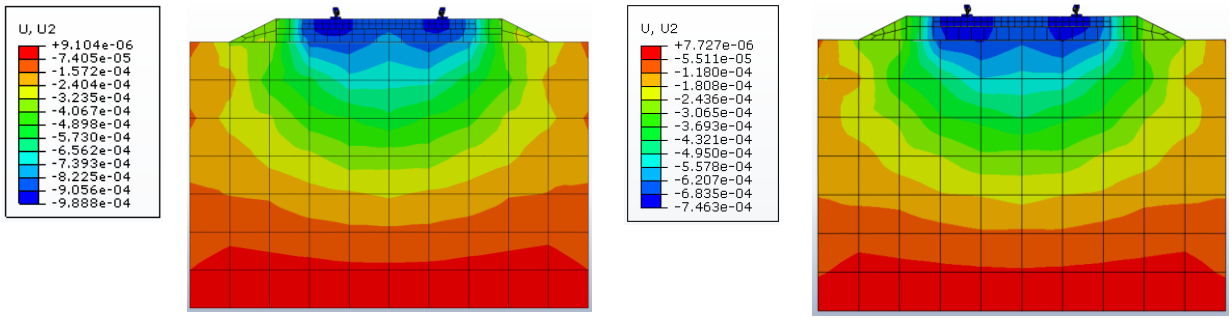

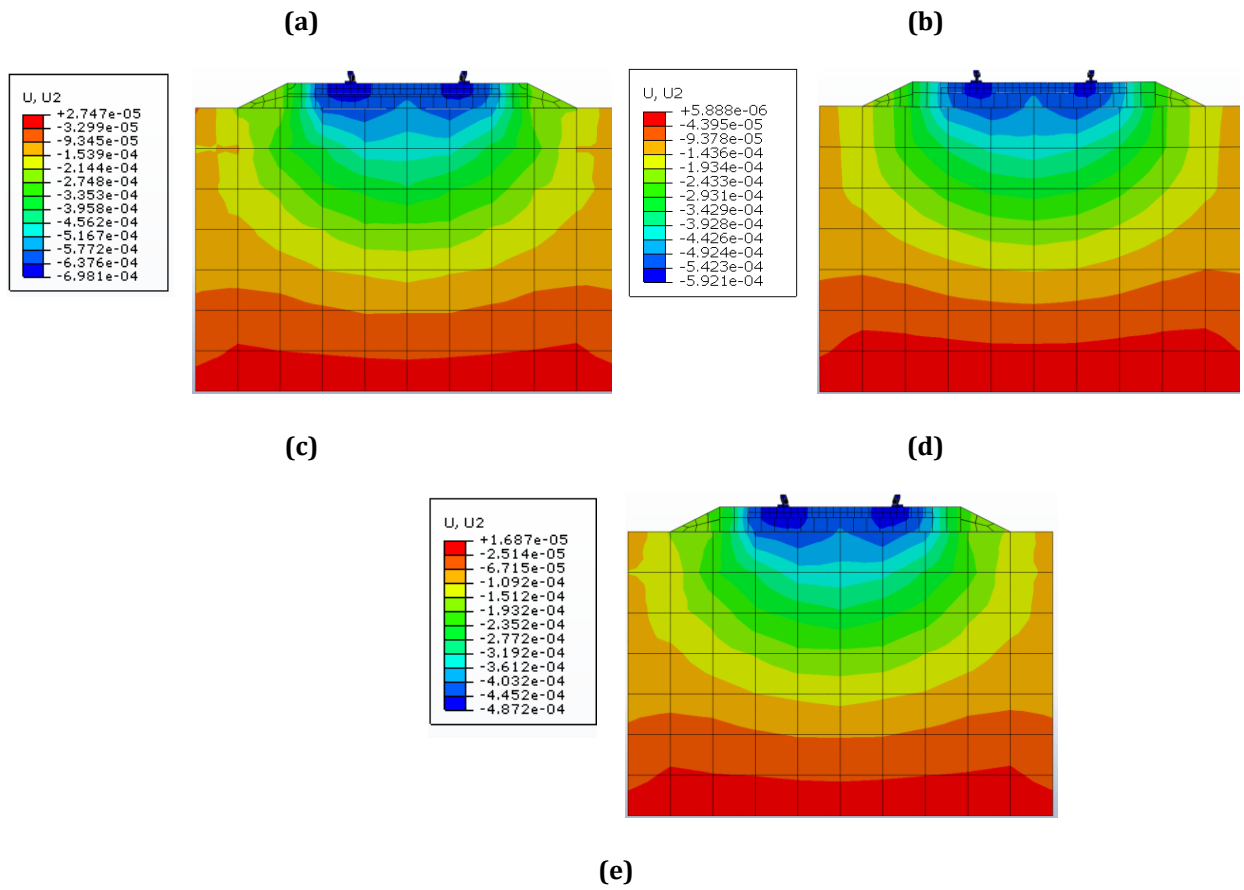

Fig. 8. The deflection of track components (m) corresponding to different ballast layers as **(a)**0%SS, **(b)**25%SS, **(C)**50%SS, **(d)**75%SS and **(e)**100%SS.

As can be seen in Table. 7, the deflection of rail has the highest value, followed by those of sleeper, ballast and subgrade. Increasing in steel slag content of ballast layer decreases the corresponding deflection of railway track components. For instance, the top surface deflection of 0%SS ballast layer as 0.85 mm decreases to 0.42 mm of 100%SS that shows the efficiency of the steel slag presence.

Table. 7. Maximum deflections of track components corresponding to different contents of SS.

Track components	Maximum Deflection values (mm) corresponding to SS percentage				
	0%SS	25%SS	50%SS	75%SS	100%SS
Rail head	0.98	0.74	0.69	0.59	0.48
Middle of Sleeper	0.9	0.68	0.63	0.54	0.44
Ballast top surface	0.85	0.64	0.6	0.49	0.42
Subgrade top surface	0.82	0.62	0.57	0.44	0.4

3.2.2. Sleepers' acceleration

Fig. 9 shows that sleeper acceleration root mean square (RMS) decreases as steel slag content increasing. Decreasing track components acceleration is important because directly is in relationship with passenger riding comfort [41], furthermore, track vibration decreases track components life span and results in corresponding defects [42]. These decrease percentages for 25%SS, 50%SS, 75%SS and 100%SS compared to the combination of 0%SS are about 60%, 70%, 83% and 86%, respectively. It is caused by higher stiffness of the ballast layer that provides stiffer support modulus for the rails, which significantly effects on sleeper accelerations reduction.

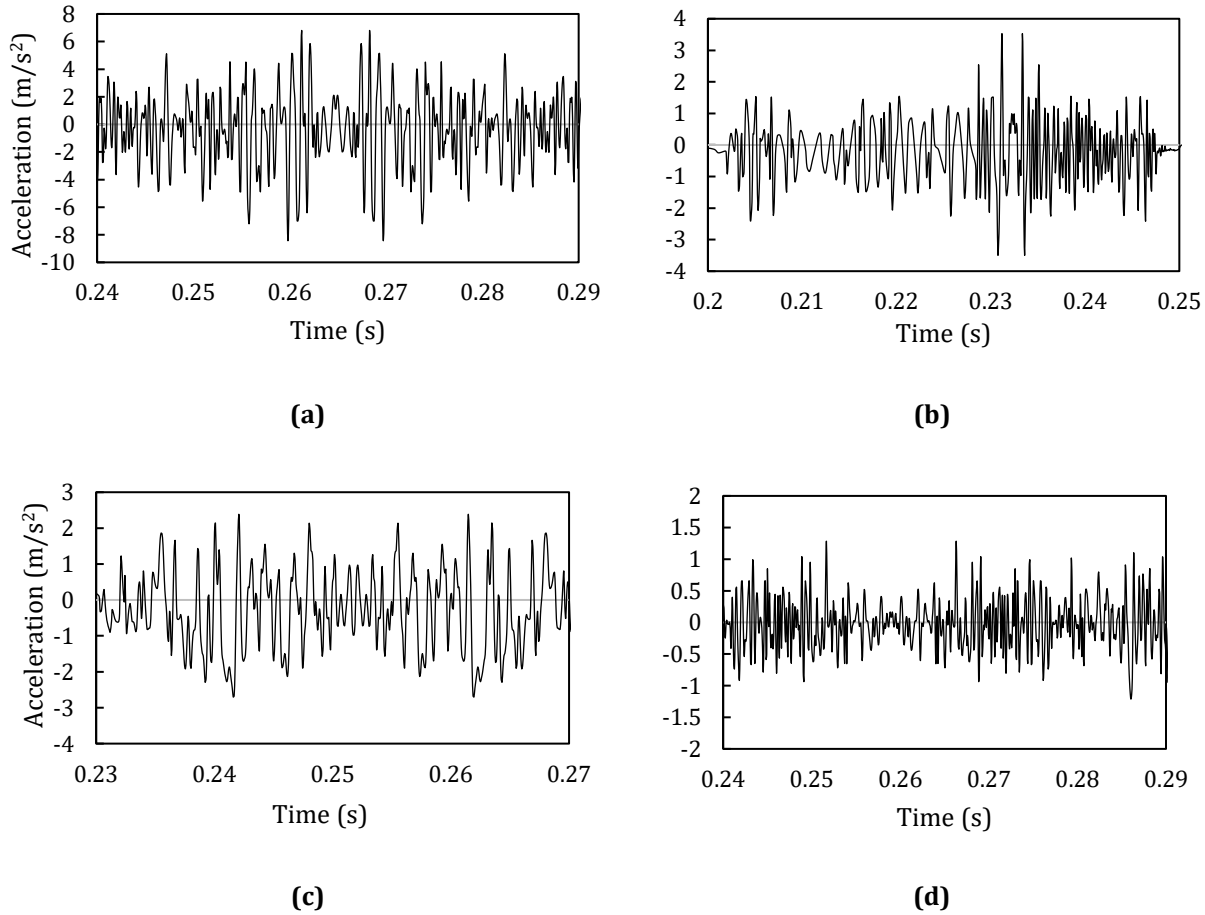

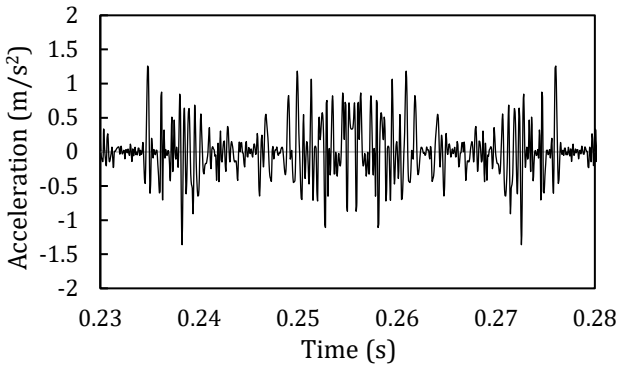

(e)

Fig. 9. Acceleration of sleeper for each different ballast layer as **(a)** 0%SS, **(b)** 25%SS, **(c)** 50%SS, **(d)** 75%SS, **(e)** and 100%SS.

Regarding the higher elasticity modulus of steel slag based on Table. 3, it was expected that higher content of steel slag shows better performance in the reduction of track acceleration. It is further proved through Table. 8, considering the RMS value of sleeper acceleration (2.08 m/s^2) in 0%SS ballasted track, it decreases to 0.75, 0.617, 0.343 and 0.276 for 25%SS, 50%SS, 75%SS and 100%SS content, respectively.

Table. 8. Different Acceleration RMS of ballast layers with different SS content.

Acceleration of sleeper	Different SS percentages of ballast layers				
	0%SS	25%SS	50%SS	75%SS	100%SS
RMS value	2.08	0.75	0.617	0.343	0.276

3.2.3. Ballast layers' damping ratios

In this section, one of the dynamical properties of railway ballasted track is measured. This parameter for ballast layer can be obtained using ballast box test [5] or field measurement of ballast vibration [43]. In this regards, the free vibration response of railway track acceleration is selected as follows in Fig. 10. Five consecutive acceleration values are chosen

to be used in Equation (4). Using Equation (3), the damping ratio of ballast layer can be achieved.

$$\zeta = \frac{\delta}{\sqrt{4\pi^2 + \delta^2}} \tag{3}$$

$$\delta = \frac{1}{n}\log\left(\frac{A(t_0)}{A(t_n)}\right) \tag{4}$$

Where $A(t_n)$ and $A(t_0)$ are the accelerations at the *nth* peak at neighboring accelerations and δ is the logarithmic decrement of accelerations.

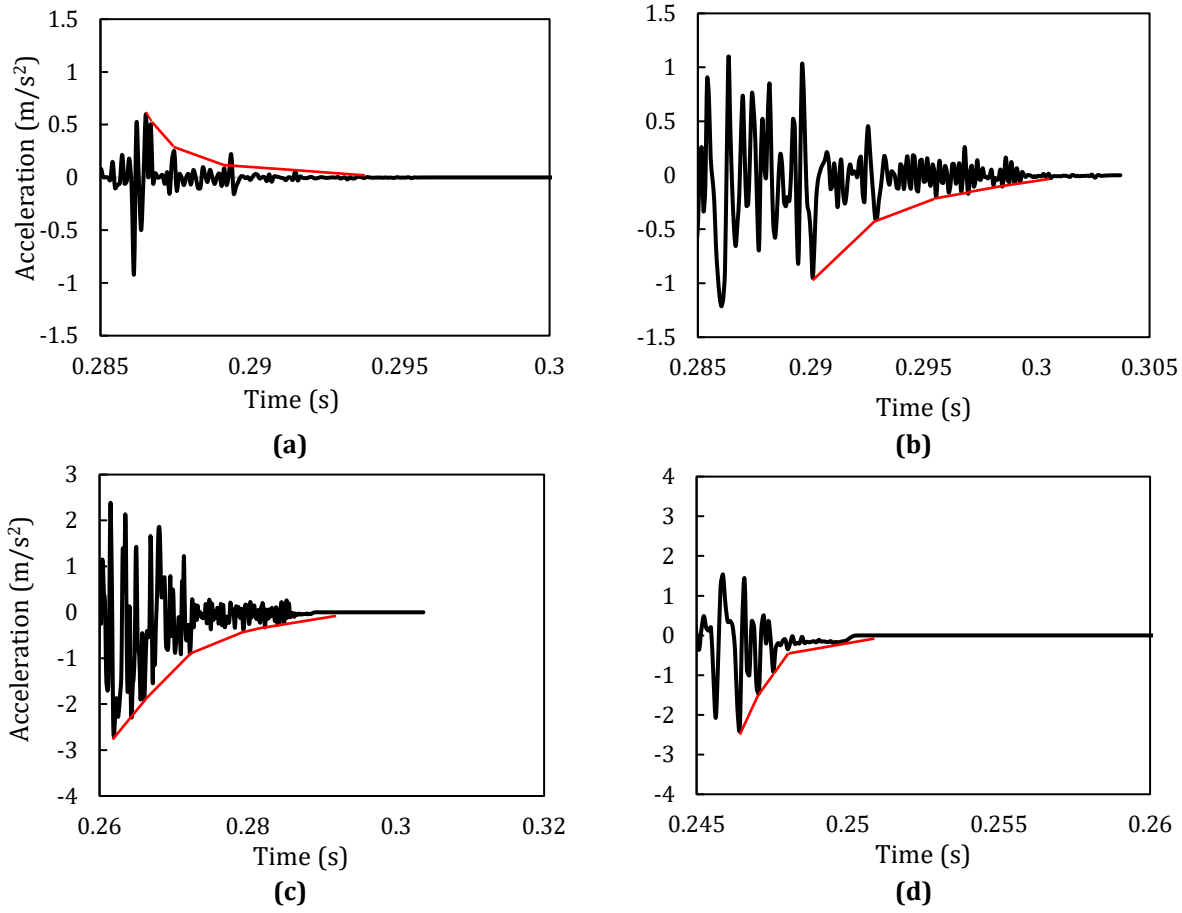

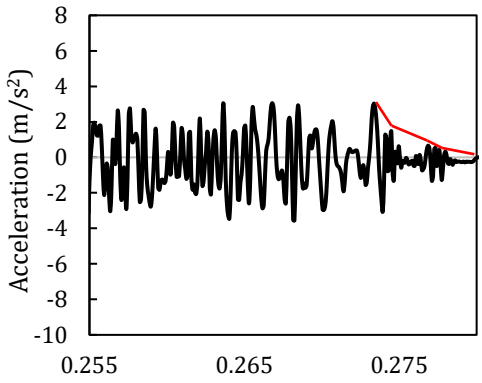

(e)

Fig. 10. Using free vibration to obtain damping ratios for **(a)** 0%SS, **(b)** 25%SS, **(c)** 50%SS, **(d)** 75%SS, **(e)** and 100%SS.

Table. 9 shows that the damping ratio of ballast decreases with increasing in steel slag content. The minimum amount of damping ratio belongs to 0%SS as 0.14 that is increased to 0.17, 0.187, 0.218 and 0.25 for 25%SS, 50%SS, 75%SS and 100%SS, respectively.

Table. 9. Different damping ratios of ballast layers with different SS content.

Damping ratio of ballast layer	Different SS percentages of ballast layers				
	0%SS	25%SS	50%SS	75%SS	100%SS
ζ	0.14	0.17	0.187	0.218	0.25

3.3. Dominant Frequencies

To compare the behavior of railway track in the frequency domain, the dominant frequencies of each ballast layer with steel slag content are obtained using Fast Fourier Transform (FFT) [44] as shown in Fig. 11. As can be seen, the dominant frequency of ballast layer with 0%SS is 10 Hz and it increases around 26% and 40% in the combinations of 25%SS and 50%SS, while it decreases around -50% and -20% in the combinations of 75%SS and 100%SS. These increase trends for 25%SS and 50%SS ballast layers means that according to the equation of natural frequency ($\omega = \sqrt{\frac{k}{m}}$), the increase in stiffness compared to the increase in the mass

of the whole railway track is more, which, consequently, increases the dominant frequencies of ballast layers. On the other hand, for 75%SS and 100%SS ballasted railway tracks, the amount of increase in weight of the whole track is higher than track increase in stiffness which results in decreasing dominant frequencies of ballast layers. Overall, the reduction of dominant frequencies less than around 10 Hz for railway track is more convenient in case of preventing track resonance and safely train passage [37] which is more discussed in the following section.

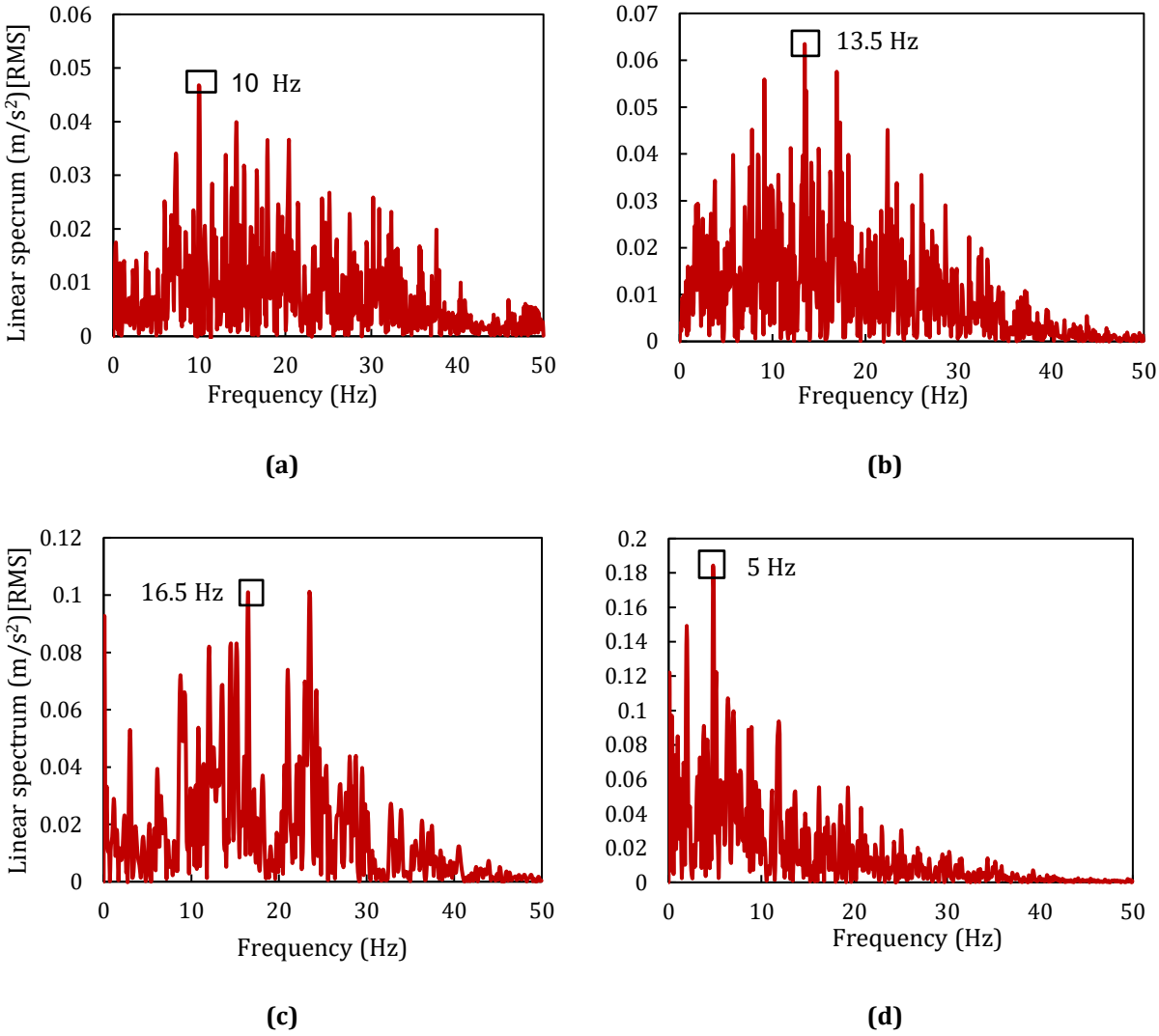

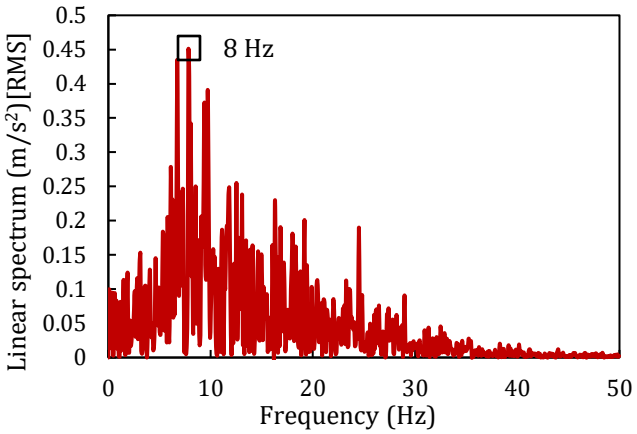

(e)

Fig. 11. The dominant frequencies of each ballasted track including **(a)** 0%SS, **(b)** 25%SS, **(c)** 50%SS, **(d)** 75%SS and **(c)** 100%SS.

3.4. Results and discussion

Table. 10 presents the comparison between ballast layers consisted of 25%SS, 50%SS, 75%SS and 100%SS compared to 0%SS ballast layer. This comparison includes four main results as maximum rail deflection, RMS values of sleeper acceleration, railway ballast combinations' damping ratios and dominant frequencies of each ballast layer under dynamic loading by heavy haul train. By comparing rail deflections of stone ballast-steel slag combinations it can be concluded that 100%SS ballast layer has the minimum deflection which is followed by 75%SS, 50%SS, 25%SS and 0%SS, which means that it can lead to a longer period of maintenance and preventing ballast track components' defects. Moreover, sleeper acceleration with the presence of steel slag significantly decreases, which results in lower ballast breakage and keeps the performance of ballasted track in the efficient state. Thus, it means that steel slag can provide relatively higher damping feature for ballast layer as is shown in Table. 10 that damping ratio of 25%SS ballast layer compared to 0%SS increases by 18% as well as 50%SS, 75%SS and 100%SS that increase by 25%, 36% and 44%, respectively.

Trains often produce significant noise and vibration within a wide range of frequencies [45-48]. But the relatively low-frequency range between 10 Hz and 300 Hz seems to be of particular significance in excitation frequencies range made by wheel sets. In heavy haul trains are particularly relevant for the life span of train's parts and track components [49]. Therefore, the highlighting has been placed on the possibility of coincidence in characteristic frequencies in this frequency band of 10 Hz to 300 Hz. The decrease in dominant frequencies of ballasted railway track can lead to less possibility of coincidence of excitation frequency and track system frequency and avoiding the resonance of which that reduces the travel comfort index of passengers. Considering that, increasing steel slag content can improve ballast layer performance, it is expected that 100%SS content can be the best option, but frequency domain analysis shows that 75%SS ballast layer can be even a better choice due to lower dominant frequency.

Table. 10. Results of FEM models with different ballast layers.

Results of maximum values	Ballast layers								
	0%SS	25%SS		50%SS		75%SS		100%SS	
	Value	Value	Difference (%)	Value	Difference (%)	Value	Difference (%)	Value	Difference (%)
Rail deflection (mm)	0.98	0.74	24	0.69	30	0.59	40	0.48	51
Sleeper acceleration RMS (m/s^2)	2.08	0.75	60	0.617	70	0.343	83	0.276	86
Ballast damping ratio	0.14	0.17	18	0.187	25	0.218	36	0.25	44
Dominant frequency (Hz)	10	13.5	26	16.5	40	5	-50	8	-20

4. Conclusions

This research aims to investigate the behavior of the ballast layer consisted of different fractions of stone ballast mixed by steel slag particles using the finite element method. In this regard, the elasticity modulus and Moher-Coulomb properties of five fractions of 0%, 25%, 50%, 75% and 100% Steel slag by weight of ballast obtained by shear strength and plate load tests which were used as ballast layer properties for the FEM modeling. Five different SB-SS combinations as ballast layer were developed in a numerical model and the behavior of which were assessed. Finally, railway tracks behavior were determined and compared, including rail displacement, sleeper acceleration, ballast damping ratios and dominant frequencies. The highlighted results are presented as follows:

1. The experimental results show a significant improvement in ballast layer performance by increasing steel slag percentage. The elasticity modules of the combinations of 25%SS, 50%SS, 75%SS and 100%SS increase by 6.5%, 9%, 11% and 12% than that of 0%SS specimen, respectively, these increasing percentages show better mechanical performance of steel slag ballast layer under dynamic loading.
2. The displacements of rail decrease by 24%, 30%, 30% and 51% for 25%SS, 50%SS, 75%SS and 100%SS ballast layers compared to the combination of 0%SS, respectively. These decrease percentages of rail displacement further results in less ballast abrasion and track deflection.
3. Steel slag content can decrease the acceleration of track components. For instance, the sleeper acceleration for railway tracks containing 25%SS, 50%SS, 75%SS and 100%SS shows about 60%, 70%, 83% and 86% decrease, respectively. Consequently, Steel slag content of ballast layer increases passenger riding comfort and increase life span of track components.

4. Ballast damping ratio of 100%SS ballast layer is around 0.25 that is 44% more than 0%SS ballast layer. Increasing steel slag content increases damping ratios of 25%SS, 50%SS and 75%SS as 0.17, 0.187 and 0.218, respectively. This shows that the better capability of steel slag ballast layer in mitigation of vibration induced by train.
5. The presence of steel slag in ballasted railway track increases the dominant frequencies in the combinations of 25%SS and 50%SS as 26% and 40% compared to 10 Hz frequency of 0%SS. Although the dominant frequencies in the combinations of 75%SS and 100%SS ballast layers decrease as -50% and -20%, respectively, it can be concluded that frequencies of 75%SS and 100%SS are out of excitation frequency range made by train wheel sets.
6. Regarding both time and frequency histories results, 75%SS ballast layer is selected as the optimal steel slag combination with 5 Hz dominant frequency, 0.218 damping ratio, 83% sleeper acceleration reduction and 40% rail deflection reduction.

Acknowledgement

The paper was supported by China Academy of Railway Science foundation (Grant No. 2018YJ043).

Conflict of Interest

None.

References

[1] Y. Guo, V. Markine, X. Zhang, W. Qiang, and G. Jing, "Image analysis for morphology, rheology and degradation study of railway ballast: A review," *Transportation Geotechnics,* vol. 18, pp. 173-211, 2019.

[2] M. Esmaeili, K. Yousefian, and R. Nouri, "Vertical load distribution in ballasted railway tracks with steel slag and limestone ballasts," *International Journal of Pavement Engineering,* vol. 20, no. 9, pp. 1065-1072, 2019.
[3] W. Jia, V. Markine, Y. Guo, and G. Jing, "Experimental and numerical investigations on the shear behaviour of recycled railway ballast," *Construction and Building Materials,* vol. 217, pp. 310-320, 2019.
[4] B. G. Delgado, A. V. da Fonseca, E. Fortunato, and P. Maia, "Mechanical behavior of inert steel slag ballast for heavy haul rail track: Laboratory evaluation," *Transportation Geotechnics,* vol. 20, p. 100243, 2019.
[5] M. Esmaeili, P. Aela, and A. Hosseini, "Experimental assessment of cyclic behavior of sand-fouled ballast mixed with tire derived aggregates," *Soil Dynamics and Earthquake Engineering,* vol. 98, pp. 1-11, 2017.
[6] M. Sol-Sánchez, F. Moreno-Navarro, M. Rubio-Gámez, N. Manzo, and V. Fontseré, "Full-scale study of Neoballast section for its application in railway tracks: optimization of track design," *Materials and Structures,* vol. 51, no. 2, p. 43, 2018.
[7] K. Horii, N. Tsutsumi, Y. Kitano, and T. Kato, "Processing and reusing technologies for steelmaking slag," *Nippon Steel Tech Rep,* vol. 104, no. 104, pp. 123-29, 2013.
[8] F. Maghool, A. Arulrajah, S. Horpibulsuk, and Y.-J. Du, "GEOTECHNICAL PROPERTIES OF LADLE FURNACE SLAG IN ROADWORK APPLICATIONS," in *Sixth International Conference on Geotechnique, Construction Materials and Environment, Bangkok, Thailand*, 2016.
[9] B. Björkman, "Activity: European Slag Conference; Euroslag 2010," in *European Slag Conference: 20/10/2010-22/10/2010*, 2010.
[10] J. Bowyer *et al.*, "Understanding steel recovery and recycling rates and limitations to recycling," *Dovetail Partners Inc.: Minneapolis, MN, USA,* pp. 1-12, 2015.
[11] J. Guo, Y. Bao, and M. Wang, "Steel slag in China: Treatment, recycling, and management," *Waste management,* vol. 78, pp. 318-330, 2018.
[12] M. Esmaeili, S. Ataei, and M. Siahkouhi, "A case study of dynamic behaviour of short span concrete slab bridge reinforced by tire-derived aggregates as sub-ballast," *International Journal of Rail Transportation,* pp. 1-19, 2019.
[13] P. K. Chamling, S. Haldar, and S. Patra, "Behavior of Steel Slag Ballast for Railway under Cyclic Loading."
[14] M. Morata, C. Saborido, and V. Fontserè, "Slag aggregates for railway track bed layers: Monitoring and maintenance," *Computers in Railways XV: Railway Engineering Design and Operation,* vol. 162, p. 283, 2016.
[15] M. Kaya, "A study on the stress-strain behavior of railroad ballast materials by use of parallel gradation technique," *The Middle East Technical University. http://etd. lib. metu. edu. tr/upload/3/12605026/index. pdf,* 2004.
[16] M. Esmaeili, R. Nouri, and K. Yousefian, "Experimental comparison of the lateral resistance of tracks with steel slag ballast and limestone ballast materials," *Proceedings of the Institution of Mechanical Engineers, Part F: Journal of Rail and Rapid Transit,* vol. 231, no. 2, pp. 175-184, 2017.
[17] M. Esmaeili, K. Yousefian, and P. Asgharzadeh Ghahroudi, "An investigation of abrasion and wear characteristics of steel slag and granite ballasts," *Proceedings of the Institution of Civil Engineers-Construction Materials,* vol. 173, no. 1, pp. 41-52, 2020.
[18] J. Sahay, O. Nagpal, and S. Prasad, "Waste management of steel slag," *Steel times international,* vol. 24, no. 2, p. 38, 2000.
[19] T. Koh, S.-W. Moon, H. Jung, Y. Jeong, and S. Pyo, "A Feasibility Study on the Application of Basic Oxygen Furnace (BOF) Steel Slag for Railway Ballast Material," *Sustainability,* vol. 10, no. 2, p. 284, 2018.
[20] Y. N. Dhoble and S. Ahmed, "Review on the innovative uses of steel slag for waste minimization," *Journal of Material Cycles and Waste Management,* vol. 20, no. 3, pp. 1373-1382, 2018.
[21] E. A. Oluwasola, M. R. Hainin, and M. M. A. Aziz, "Characteristics and utilization of steel slag in road construction," *Jurnal Teknologi,* vol. 70, no. 7, pp. 117-123, 2014.
[22] G. Wang, "Properties and utilization of steel slag in engineering applications. Wollongong," Ph. D. Thesis, University of Wollongong, 1992.
[23] L. Le Pen, W. Powrie, A. Zervos, S. Ahmed, and S. Aingaran, "Dependence of shape on particle size for a crushed rock railway ballast," *Granular Matter,* vol. 15, no. 6, pp. 849-861, 2013.
[24] S. Ahmed, J. Harkness, L. Le Pen, W. Powrie, and A. Zervos, "Numerical modelling of railway ballast at the particle scale," *International Journal for Numerical and Analytical Methods in Geomechanics,* vol. 40, no. 5, pp. 713-737, 2016.

[25] M. Esmaeili, A. Khodaverdian, H. K. Neyestanaki, and S. Nazari, "Investigating the effect of nailed sleepers on increasing the lateral resistance of ballasted track," *Computers and Geotechnics,* vol. 71, pp. 1-11, 2016.
[26] B. Indraratna, N. T. Ngo, C. Rujikiatkamjorn, and J. Vinod, "Behavior of fresh and fouled railway ballast subjected to direct shear testing: discrete element simulation," *International Journal of Geomechanics,* vol. 14, no. 1, pp. 34-44, 2014.
[27] A. Danesh, M. Palassi, and A. A. Mirghasemi, "Effect of sand and clay fouling on the shear strength of railway ballast for different ballast gradations," *Granular Matter,* vol. 20, no. 3, p. 51, 2018.
[28] Z. Wang, G. Jing, Q. Yu, and H. Yin, "Analysis of ballast direct shear tests by discrete element method under different normal stress," *Measurement,* vol. 63, pp. 17-24, 2015.
[29] X. Bian, W. Li, Y. Qian, and E. Tutumluer, "Micromechanical particle interactions in railway ballast through DEM simulations of direct shear tests," *International Journal of Geomechanics,* vol. 19, no. 5, p. 04019031, 2019.
[30] A. R. TolouKian, J. Sadeghi, and J.-A. Zakeri, "Large-scale direct shear tests on sand-contaminated ballast," *Proceedings of the Institution of Civil Engineers-Geotechnical Engineering,* vol. 171, no. 5, pp. 451-461, 2018.
[31] A. Manual, "American Railway Engineering and Maintenance-of-Way Association," 2006.
[32] S. Timoshenko, "P, and Goodier, JN Theory of Elasticity," ed: McGraw Hill, 1970.
[33] J. Boussinesq, "Discussed in Theory of Elasticity," ed: McGraw-Hill, NY (1970), 1885.
[34] A. D. Kerr, *Fundamentals of railway track engineering*. 2003.
[35] J. Sadeghi, H. Liravi, and M. H. Esmaeili, "Experimental investigation on loading pattern of railway concrete slabs," *Construction and Building Materials,* vol. 153, pp. 481-495, 2017.
[36] Abaqus, "ABAQUS user's manual. Version 6.14," ed: Abaqus Providence, RI, 2014.
[37] M. Esmaeili and M. Siahkouhi, "Tire‐derived aggregate layer performance in railway bridges as a novel impact absorber: Numerical and field study," *Structural Control and Health Monitoring,* vol. 26, no. 10, p. e2444, 2019.
[38] S. Ataei, M. J. Alikamar, and V. Kazemiashtiani, "Evaluation of axle load increasing on a monumental masonry arch bridge based on field load testing," *Construction and Building Materials,* vol. 116, pp. 413-421, 2016.
[39] A. Standard, "Methods for sampling and testing aggregates," ed: Method, 2009.
[40] M. Heelis, A. Collop, A. Dawson, D. Chapman, and V. V. Krylov, "Predicting and measuring vertical track displacements on soft subgrades," 1999.
[41] J. Sadeghi, "Field investigation on vibration behavior of railway track systems," 2010.
[42] P. A. Ferreira and A. López-Pita, "Numerical modelling of high speed train/track system for the reduction of vibration levels and maintenance needs of railway tracks," *Construction and Building Materials,* vol. 79, pp. 14-21, 2015.
[43] M. Ülker-Kaustell and R. Karoumi, "Influence of non-linear stiffness and damping on the train-bridge resonance of a simply supported railway bridge," *Engineering Structures,* vol. 41, pp. 350-355, 2012.
[44] A. Brandt, *Noise and vibration analysis: signal analysis and experimental procedures*. John Wiley & Sons, 2011.
[45] A. Wang and S. Cox, "High-speed rail: excitation frequencies and track stiffness," in *Noise and Vibration Mitigation for Rail Transportation Systems*: Springer, 2012, pp. 151-158.
[46] A. Wang and S. Cox, "Noise characteristics of high speed track with railpads of different stiffness," in *Proceedings of EuroNoise*, 1998, pp. 295-300.
[47] S. Cox and A. Wang, "Effects of rail fastening on railway track noise," in *INTER-NOISE and NOISE-CON Congress and Conference Proceedings*, 2000, vol. 2000, no. 6, pp. 2387-2394: Institute of Noise Control Engineering.
[48] A. Wang and S. Cox, "Effect of rail pad stiffness on rail roughness growth and wayside noise levels on high speed track," in *The 6th World Congress on Railway Research, Edinburgh, UK*, 2003.
[49] H. Koh, H. Kwon, W. You, and J. Park, "A study on source mechanism in the interior noise problem of high speed trains," in *Noise and Vibration Mitigation for Rail Transportation Systems*: Springer, 2008, pp. 222-228.